Atmos. Meas. Tech. Discuss., doi:10.5194/amt-2016-76, 2016
Manuscript under review for journal Atmos. Meas. Tech.
Published: 18 March 2016

Atmospheric Measurement Techniques Discussions

Airborne laser scan data: a valuable tool to infer partial beam-blockage in urban environment

Roberto Cremonini[1,3], **Dmitri Moisseev**[1,4], **and V. Chandrasekar**[1,2]

[1]Department of Physics, University of Helsinki, Helsinki, Finland
[2]Colorado State University, Fort Collins, Colorado
[3]ARPA Piemonte, Dipartimento Sistemi Previsionali, Turin, Italy
[4]Finnish Meteorological Institute, Helsinki, Finland

Correspondence to: Roberto Cremonini (rcremoni@mappi.helsinki.fi)

Abstract. High spatial resolution weather radar observations are of primary relevance for hydrological applications in urban areas. However, when weather radars are located within metropolitan areas, partial beam blockages and clutter by buildings can seriously affect the observations. Standard simulations with simple beam propagation models and digital elevation models (DEMs) are usually not able to evaluate the buildings contribution to partial beam blockages. In the recent years airborne laser scanners (ALS) evolved to the state-of-the-art technique for topographic data acquisition. ALS data, providing small footprint diameters (10 – 30 cm), allow accurate reconstruction of buildings and forest canopy heights. Analyzing the three weather C-band radars located in the metropolitan area of Helsinki, Finland, the present study investigates the benefits of using ALS data for quantitative estimations of partial beam blockings. The results obtained applying beam standard propagation model are compared with stratiform 24-hour rainfall accumulation to evaluate the effect of partial beam blocking due to the constructions and trees. To provide the physical interpretation of the results, the detailed analysis of beam occultations is achieved by open spatial data sets and interface services with open source Geographic Information Systems.

1 Introduction

Rapid, uncontrolled spatial growth and densification create settlements in inappropriate areas most likely to be exposed to natural hazards. In 2014, about 54 per cent of the world's population lived in urban areas (United Nations, 2014), with an increase from 43% in 1990. According to the UNISDR (2011), over 80% of disasters reported by national sources occurred in urban areas. Moreover, in 2014, nearly 56% of cities, representing 62% of city inhabitants worldwide, were at high risk of exposure to at least one type of natural disaster. As reported in the CRED/OFDA International Disaster Database (Guha-Sapir et al, 2016), hydro-meteorological hazards (floods, cyclones and storms) are the most relevant types. Einfalt et al (2004) reported several applications of weather radar rainfall to urban hydrology demonstrating widespread increasing of weather radar observations in urban environment. However, recent studies demonstrated that up to 100-meters resolution quantitative precipitation estimation (QPE) and 1-minute scans are required in order to be useful for pluvial flood forecast in urban environment (Berne et al (2004), Veldhuis et al (2014)). As the spatial resolution of weather radar observations decreases with the distance from the antenna, for urban hydrology the sensor can not be placed too far from the target area. But, when the weather radar is located within urbanized areas, buildings, masts and trees produce several partial beam blockages (PBBs) and large return clutter. Beam occultations lead to an underestimation of precipitation rate, especially in winter conditions when the upper part of the radar volume is filled by snow and ice crystals. Therefore, the identification of areas where the radar quantitative precipitation estimation is affected by PBBs is mandatory for successful hydrological applications in urbanized areas. Several beam blockage correction schemes can be applied in order to minimize the effect of PBBs on QPEs (Kitchen et al (1994); Fulton et al (1998); Bech et al (1968); Lang et al (2009)). The developing of polarimetry has also demonstrated that QPEs based on the specific propagation phase (KDP) are rel-

Atmos. Meas. Tech. Discuss., doi:10.5194/amt-2016-76, 2016
Manuscript under review for journal Atmos. Meas. Tech.
Published: 18 March 2016

Atmospheric Measurement Techniques Discussions

atively insensible to partial beam-blockages (Giangrande and Ryzhkov, 2005). However, PBB-correction schemes based on KDP cannot be applied when radar observations are in snow or ice (Zhang et al, 2013) and, moreover, many operational weather radar are still in single polarization. As demonstrated in several studies (Kucera et al (2004); Fornasiero et al (2006); Krajewski et al (2006)), accurate radar visibility maps can be obtained applying beam standard atmospheric propagation model (Doviak and Zrnic, 1984) coupled with high resolution digital elevation models (DEMs). Furthermore, Krajewski et al (2006) also demonstrated that PBBs can be successfully estimated by modelling radar visibility using accurate DEMs data and Geographic Information Systems (GIS). Unfortunately, buildings, infrastructures (masts, power-lines) and forest canopy are not represented in DEMs by definition; therefore, the estimated radar visibility in urban areas tends to be optimistic, missing heavy beam blockages due to obstacles close to the radar antenna. In the recent years LiDAR (light detection and ranging or laser induced direction and ranging) technology is proving to be the most promising data source to fill the gap between DEMs and actual surfaces. Recently, airborne laser scanning (ALS) data, the state-of-the-art technique for topographic data acquisition, provide small footprint diameters (10 - 30 cm), that allows accurate estimations of buildings, constructions and forest canopy heights (Shan et al, 2008). In this paper the PBBs of Helsinki, Finland, C-band weather radar network, are evaluated. This study investigates the benefits of using ALS data in metropolitan areas respect to DEMs for quantitative estimations of radar beam occultations. Finally, the physical interpretation of the results are obtained analyzing data by open data, provided by the Finnish publishing platform AAVA (http://avaa.tdata.fi/web/avaa/tietoa-palvelusta), and open source GIS interfaces. Section 2 outlines the radar data, ALS dataset and the methodology used. The discussion of the results and the conclusions are presented respectively in Section 3 and 4.

2 Data and methodology

Laser scanning or LiDAR offers the most accurate method for collecting elevation data for the production of digital elevation or surface models. Airborne laser scanning is a rapid, highly accurate and efficient method of capturing 3D data of large areas, such as agricultural or forestry sites, urban areas, industrial plants, etc.; its development goes back to the 1970s and 1980s, with an early NASA system and other attempts in USA and Canada (Ackermann et al, 1999). The benefits of ALS data consist in significantly improved accuracy, lower processing costs and higher automation, and, thus, performing national laser scanning are already completed or planned in many countries. For example, in Germany large parts of the country has been scanned and the work is going on federal basis. The National Land Survey of Finland (NLS) began collecting airborne laser scanning data throughout Finland in 2008 to provide a new high-detailed terrain elevation model. The Finnish ALS data are organized in 3-km by 3-km tiles with an average points density of about 1.2 per meter square. According to Ahokas and Kaartinen (2013), the ALS accuracy obtained in all various surface types was better than 30 cm (RMSE). ALS data are geo-located using the ETRS89 – ETRS-TM35FIN geographical coordinate system. Since 2005 the Finnish Meteorological Institute (FMI) and Vaisala Oyj have established and maintained the high resolution mesoscale network called Helsinki Testbed (http://testbed.fmi.fi/). The aim was to develop an internationally recognized platform where scientists could deploy their measurement devices and monitor small-scale weather phenomena (Koskinen et al, 2014). Recently, Helsinki UrBAN (Urban Boundary-layer Atmosphere Network, http://urban.fmi.fi) project has started a long-term intensive observational network to study physical processes in the atmosphere above the city (Wood et al, 2013). The network's key purpose is the understanding of the physical processes in the urban boundary layer such as fluxes of heat, momentum, exchanges of water vapour. Within this research context, three dual-polarization C-band weather radar operate in the Helsinki metropolitan area. The Figure 1 shows the weather radar location and the urban area of Helsinki. The Vantaa weather radar (hereafter VAN) is operated by the Finnish Meteorological Institute (FMI) and it has been installed on the old water tower of Vantaa's Kaivoksela, close to the city international airport (Saltikoff and Nevvonen, 2011). The Kumpula radar (KUM) is operated by the Department of Physics of University of Helsinki (UHEL) and it is located on the roof of the main building of the Kumpula campus, about 4 km north-east from the city center. Last, the Kerava radar (KER) is located northward about 23 km far from the city centre, operated by Vaisala Oyj, and it is used for research purposes by the UHEL radar meteorology group. Given the antenna resolution and the relatively short distance between the radar sites, these instruments can provide rainfall estimations for the city of Helsinki with the satisfactory spatial resolution required hydrological and hydraulic models. The antenna pointing accuracy for the three weather radar is about 0.1° and their lowest elevations of the operational scans are 0.4° and 0.7° elevation for VAN and KER and 0.5° and 1.0° elevation for KUM. The Table 1 summarizes the weather radar locations and their main characteristics.

2.1 Methodology

ALS data consist of geo-located points (about 7 - 5 million per tile), reporting the surface height. The Figure 2 shows ALS tiles used in the analysis. These points have to be projected from their native map projection to radar-centric coordinates system, i.e. azimuth from north and slant range from the antenna. ALS points lower than the base of the antenna have been discharged as negative elevations are not used by

Atmos. Meas. Tech. Discuss., doi:10.5194/amt-2016-76, 2016
Manuscript under review for journal Atmos. Meas. Tech.
Published: 18 March 2016

Atmospheric Measurement Techniques Discussions

the three Helsinki radars. Ultimately, ALS data have been visually inspected to remove isolated and suspected points. When the beam intercepts an obstacle, then beam occultation occurs. Using beam *"atmospheric standard propagation"* equations, it is possible to derive the height of the beam respect to the surface, given the elevation and the azimuth. Recalling Doviak and Zrnic (1984), the height of the center of the beam h, leaving the radar with elevation θ_e, is given by the well-known equation:

$$h = k_e[\frac{cos\theta_e}{cos(\theta + s/k_e a)}] \quad (1)$$

while the following two equations relate r and θ_e:

$$h = [r^2 + (k_e a)^2 + 2rk_e a sin\theta]^{1/2} - k_e a \quad (2)$$

$$s = k_e a sin^{-1}(\frac{rcos\theta_e}{k_e a + h}) \quad (3)$$

where r is the great circle distance from the antenna and s the slant range; k_e depends on the refractivity gradient, which is function of atmospheric temperature, humidity and pressure. Observations demonstrate that the refractive index gradient in the first one or two kilometers of the atmosphere is often constant, so the effective radius $k_e a$ is approximately $\frac{4}{3}a$: these conditions are usually referred as *"standard propagation conditions"*. Inverting Equations 1,2 and 3, it is also possible to obtain the ground range (great circle distance), the height above the Earth's surface given the slant range (along the beam) and the elevation angle. Given a surface profile in the field-of-view of the radar, the faction of blocked beam has to be derived to estimate the beam occultation.
Although the antenna pattern is usually complex, assuming a symmetrical antenna with all energy focused in the main lobe is a common approximation to calculate the integral of the total emitted power. Considering a two-dimensional Gaussian illumination function, the antenna radiation pattern is given by

$$f(\phi) = exp[-ln(2)(\frac{\phi}{\phi_{3dB}})^2] \quad (4)$$

where ϕ_{3dB} is the angular separation in which the magnitude of the radiation pattern decreases by 50% (or -3 dB) and it is named half-power beamwidth. The angle ϕ is measured from the point of maximum radiation. The beam propagation has been modelled dividing the beam in rays varying azimuth and elevation in the range of 3-dB width and applying the Equations 1, 2 and 3: the emitted power for each ray is given by $f(\phi)$ multiplied by P_0 (the emitted power in the center of the beam). When the obtained ray height is lower than ALS points, the beam is considered blocked. The total expected blocking is derived as the ratio between emitted power weighted unblocked and blocked rays. After having obtained the PBB estimations, the results are checked locating the obstacles by GIS interface QGIS (2015), web mapping (AAVA Open data, Google Maps and OpenStreetmap) and by evaluation their pictures.

3 Results

The described processing has been implemented for Kumpula, Vantaa and Kerava radar to estimate at lowest elevations the partial beam-blockages caused by buildings, trees or masts. Hereafter, overall results are reported and specific cases are analyzed for each weather radar of Helsinki network.

Kumpula weather radar
Located on the roof of the University of Helsinki building in Kumpulan Campus, the radar is the closest to the city center (only about 4 km). Its lowest elevations of the operational scan are 0.5° and 1.0°. Considering 0.5° elevation, several strong partial beam-blockages occur. The strongest expected PBB happens from 169° to 170° azimuth and it is due to the huge Hanasaari power plant, 2.2 km far from the radar. This severe beam blockage is mainly caused by two power plan chimneys, one 150 meters tall with eight meters diameter, the other 100 meters tall with six meters diameter. As the antenna positioning accuracy is 0.1°, several antenna positions have been randomly generated from a uniform distribution, varying both azimuth and elevation in a range comprised between -0.1° and +0.1°. In this way, it is possible to evaluate more robustly the expected PBB and its uncertainty taking in account for the antenna positioning accuracy. At 170° azimuth, the chimneys cause 3.98 dB two-way losses with 1.18 dB inter-quantile range: this uncertainty estimation is derived sampling 100 azimuths and elevations. The other relevant PPBs happen at 192° azimuth (4.42 dB), corresponding to Paavalin Kirkko bell tower, 0.8 km far from the antenna, and between 233° and 245°, corresponding to the residential buildings in Itä-Pasila, 1.4 km far from the radar, where the occultation reaches 6.02 dB. The YLE Studiotalo buildings with their television tower cause large PBBs between 265° and 271° azimuths, up to 6.36 dB. Finally, the Linnanmäki amusement park of Helsinki at 216° azimuth causes 2.38 dB two-way losses and some minor PBBs happen between 304° and 347°: they are caused by a mast and forest canopy in The Central Park of Helsinki and by residential buildings in Käpylä.
Hereafter, as explanatory example, we focus on the occultation caused by the Paavalin Kirkko bell tower. The Figure 3 on left shows the Kumpula radar location and the bell tower located at about 0.8 km toward south. The superimposed points are ALS data. The expected partial beam blocking, derived for 0.5° elevation considering the 1.05° antenna beamwidth, is also shown in Figure 3. The colour shading represents the beam power distribution within 3-dB

Atmos. Meas. Tech. Discuss., doi:10.5194/amt-2016-76, 2016
Manuscript under review for journal Atmos. Meas. Tech.
Published: 18 March 2016

Atmospheric Measurement Techniques Discussions

beamwidth, relative to the maximum in the center. The dark blue colour shows the occultation caused by the bell tower; its shape is derived from the ALS points with a simple linear approximation. The two-way estimated beam-blockage by one hundred samples around 192° azimuth and 0.5° elevation is 4.50 dB (median value) and the inter-quantile range is 1.15 dB. As expected, rising the antenna to 1.0° elevation, the radar visibility greatly improves: some PBBs reduce to less than 1 dB, while the strongest ones sensibly decrease. The expected PBBs caused by Hanasaari power plant decrease to 2.31 dB at 169° azimuth and to 2.79 dB at 170° azimuth. Paavalin Kirkko PBB reduces to less than 1 dB, Itä-Pasila residential area PBB reaches 1.69 dB and YLE Studiotalo decreases to 5.13 dB. All PBBs for azimuths greater than 275° range disappear. The 2 summarizes the estimated partial beam-blockages, deduced by ALS data analysis, for Kumpula radar.

Vantaa weather radar

The radar (84 m above sea level) is located over the Kaivoksela water tower, in Kaivoksela, Vantaa, about 8 km far from Helsinki International Airport toward south-west. Even at lowest elevation (0.4°), the radar visibility is pretty good, except for minor PBBs between 212° and 214° (about 1 dB) azimuths, corresponding to Malminkartano hill, 90 m above sea level altitude. The main obstacle is the huge Myyrmäki water tower, a concrete tower 47 meters tall, 41-meters diameter with a capacity of 4,500 m^3. The tower is located at about 2 km at 272° azimuth (Figure 4). Repeating the above-mentioned process, that is, randomly varying one hundred times the azimuth and the elevation within the antenna positioning uncertainty, the median value of two-ways losses is 7.20 dB with 2.45 dB inter-quantile range. Rising the elevation up to 0.7° the beam occultation decreases to 2.06 dB with 0.87 dB inter-quantile range. The beam is completely free only at 1.0° elevation. An another relevant partial beam-blockage (2.7 dB with 1.07 inter-quantile range) occurs at 309° with 0.4°, corresponding to the Martinlaakson power plan, 2.3 km far from the Vantaa radar: the main responsible for this beam occultation are its four 60-meters tall chimneys. When the antenna elevation is risen to 0.7° elevation, the partial beam blockage reduces to 0.90 ± 0.22 dB.

Kerava weather radar

The Kerava weather radar, a Vaisala WRM200, is located on the top of a water tower in the town of Kerava at 95 meters above sea level. At 0.4° elevation only two partial beam-blockages (about 1.2 dB) occur at 356° azimuth, corresponding to an industrial plant 2.4 km far from the radar, and at 106° azimuth, corresponding to a mast located 0.9 km far from the radar site. Raising the antenna to 0.7° elevations, all PBBs disappear.

4 Discussion

The analysis of PBBs using airborn laser scan data in the metropolitan area of Helsinki showed that at low elevations severe beam occultations occur. This result could not be obtained from digital terrain models as they do not include trees, buildings and constructions. As shown by the weather radar PPB analysis, Kumpula is the radar site most effected by occultations caused by metropolitan buildings and constructions: for this reason hereafter we focus in this radar.
In order to verify the PBBs derived from ALS data, stratiform precipitations that interested Helsinki for several hours have been considered. On September 22, 2014, a warm front associated to a low centred over Poland moved toward east causing extended rainfall over south Finland. On the same day at 12 UTC, the radiosounding in Jokioinen (WMO code 02963) recorded the freezing level at about 1900 m above sea level. As mentioned, in the low troposphere, the beam propagation depends on the variation of the refractive index n, for dimensional reasons usually expressed in term of refractivity $N = (n-1) \times 10^6$. For microwaves, this parameter can be estimated according to Bean and Dutton (1968):

$$N = \frac{77.6}{T} \times (P + 4810\frac{e}{T}) \quad (5)$$

Where T is the dry air temperature in Kelvin degrees, P is the atmospheric pressure in $mbar$ or hPa and e is the water vapour pressure also expressed in $mbar$ or hPa. The typical values of the refractivity vertical gradient -$\frac{\partial N}{\partial z}$ are around $-40km^{-1}$. Under favorable conditions for anomaly propagation, the refractivity gradient reaches values equal or lower than $-157km^{-1}$.
Applying 5 to Jokioinen radiosounding data, it is possible verify that on September 22, 2014 there were standard atmosphere propagation conditions (-$\frac{\partial N}{\partial z} \sim -30km^{-1}$) in the lowest three kilometers.
The Figure 5 reports the total rainfall accumulation from 00 to 24 UTC on September 22, 2014 derived by the Kumpula radar 0.5° elevation horizontal reflectivity PPI. The heaviest precipitation occurred toward west and north-west of Helsinki. Along the line passing for the radar site from north-west to south-east, it is visible the *"Doppler Snake"* due to Doppler filtering of near-zero Doppler velocity data Saltikoff (2012) . Meanwhile, several partial beam blockages are evident, it is also clearly visible close to the radar the artificial enhancement of the precipitation accumulation caused by residual clutter. The total rainfall accumulation has been derived from PPI horizontal reflectivity applying the well-known relationship $Z - R$(Marshall and Palmer, 1948):

$$Z = aR^b \quad (6)$$

Where Z is the radar reflectivity in linear units, R the rainfall rate in mm/h, a and b two empirical coefficients that

Atmos. Meas. Tech. Discuss., doi:10.5194/amt-2016-76, 2016
Manuscript under review for journal Atmos. Meas. Tech.
Published: 18 March 2016

Atmospheric Measurement Techniques Discussions

here are assumed $a = 300$ and $b = 1.5$. Considering the ratio between unblocked and blocked reflectivity and applying logarithm to 6, the two-way losses can be derived from the following equation:

$$L_{db} = \frac{Z_{blocked}}{Z_{unblocked}} = b \times 10 \log_{10} \frac{R_{blocked}}{R_{unblocked}} \quad (7)$$

where L_{dB} is the total observed estimation and $Z_{blocked}$ and $Z_{unblocked}$ are now expressed in dB and where $R_{blocked}$ and $R_{unblocked}$ are evaluated behind beyond the obstacle. To determine the ratio $R_{blocked}/R_{unblocked}$, several profiles of the rainfall accumulation across the partial beam blockage has been manually selected, using QGIS interface. The strong constrain is to choose the profiles in regions of relatively uniform rainfall fields.

The 3 reports the comparison between PBBs two-way losses estimated estimated by ALS data and observed values derived from total rainfall accumulation. Although it has been considered a relatively short-time rainfall accumulation, it is evident the good agreement between expected and retrieved values. There are two exceptions at 170° azimuth (Hanasaari power plant) and between 247° and 249° azimuths (Itä-Pasila residential area). In the first occultation there is an over-estimation of the blockage, that could be caused by a rough reconstruction of the power plant using ALS data. This unsophisticated reconstruction in case of complex constructions can contribute to PBB under-estimation. Two 20-meters tall mobile masts, located over the roof of a building in Itä-Pasila, were partially detected by the airborne laser scanning survey in 2008: they are the responsible for the large under-estimation of the partial beam blockage in Itä-Pasila. The right side of Figure 6 shows the radar beam centre, ALS data and Itä-Pasila buildings. Firstly, the beam is partially occulted by Eläketurvakeskus building, then after passing close to a flag-pole, the beam centre hits the mobile mast 1: Figure 6 also shows a picture of the two mast in Itä-Pasila from Google Street View. However, the architectural complexity of buildings in Itä-Pasila and the their rough reconstruction using ALS data can also contribute to the overall under-estimation. Excluding these two cases, the agreement between estimated and observed partial beam-blockages is generally good. The normalized mean bias is 7% and the root mean square error is 1.41 dB as shown in Figure 7. While the aforementioned analysis of Kumpula radar occultation has demonstrate the validity of this methodology, this study makes evident some limitations that can affect the two-way losses estimation accuracy. Airbone laser scanning campaigns are expensive and take place rarely: in the case of Helsinki, ALS data were collected on 2008. Recent buildings and urbanization changes can remove or introduce new beam occultations, that can not be estimated. Two cases related to Kumpula radar can explain quite well how the urban development affects PBB estimations. From the daily rainfall accumulation (Figure 5), it is clearly visible a beam blocking at 62° azimuth in direction of the city Porvoo. The observed two-way losses are about 2.61 dB, but this occultation is not detected by ALS data: recent tall buildings and cranes in the Arabia District, Helsinki, 900-meters far from the Kumpula radar are responsible for this occultation. The opposite instance happens toward north: the Korskela Forsby chimney causes a partial beam-blockage at 0° azimuth both estimated from ALS data and evident in 24-hours rainfall accumulation on September 22, 2014 (Figure 5). However, this industrial plant has been lately demolished: this partial beam blockage never occurs on recent observations.

The Figure 8 shows the 360° panoramic view from the antenna tower of Kumpula radar: the main obstacles like Paavalin Kirkko bell tower, residential buildings in Itä-Pasila and YLE Studiotalo buildings with their television tower are clearly visible. The obstacle shapes have been gathered using a simple linear model; this approximation leads to under-estimations or over-estimations in case of masts or complex shape buildings. The estimated uncertainty considering the antenna pointing accuracy under standard atmospheric propagation assumption is around 1-dB for most of the obstacles: considering different atmospheric propagation or even duct conditions, this uncertainty is expected to increase.

Finally, the manually selection of rainfall profiles across the beam occultation could lead to some uncertainties. In a future work, an objective selection of these profile could be implemented on the basis of directional constraints in rainfall spatial variability evaluating the rainfall semi-variogram or the ratio of the standard deviation to the arithmetic mean depth.

5 Conclusions

Urban hydrology requires rainfall observations with high resolution in space and time and weather radar can timely provide such observations whether located close to the urban areas. However, the need of using low antenna elevations for quantitative precipitation estimation, to get radar observations close to the ground, is in contrast with widespread beam occultations caused by buildings, trees and constructions. In urban environment the weather radar visibility derived from digital elevation models, even with very high spatial resolution, underestimates partial beam blockages Zhang et al (2013). The increased availability of airborn laser scan data over metropolitan areas can overcome this limitation. Analyzing Helsinki weather radars, this study demonstrates that accurate ALS data and GIS functionality can locate azimuthal angles where partial beam blockages occur and estimates quantitatively the associated two-way losses. With an appropriate beam propagation model and a simple reconstruction of constructions and forest canopy, it is possible estimate quantitatively beam occultations, including the uncertainties relate to antenna pointing errors. The comparison between estimated PBBs and observed, derived from

Atmos. Meas. Tech. Discuss., doi:10.5194/amt-2016-76, 2016
Manuscript under review for journal Atmos. Meas. Tech.
Published: 18 March 2016

Atmospheric Measurement Techniques Discussions

24-hours stratiform rainfall accumulation has demonstrate a good agreement both qualitative, in the identification of affected azimuths, and quantitatively in two-was losses estimations. Nevertheless, the analysis has also shown some limitations of this methodology due to urban developments and / or to rough reconstruction of the obstacles. Metal mobile masts are particularly difficult to reconstruct from ALS data: to partially overcome this limit, the use of more complex algorithms (Vosselman et al (2001), Dorninger et al (2008) or Kada and McKinley (2009)) for a more accurate reconstruction of the obstacles could reduce the spread between estimated and observed two-way losses. An other source of uncertainty is due to actual atmospheric refractivity conditions as beam standard atmospheric propagation conditions have been assumed.

These results can be used to redefine the scan strategy of weather radar located in urban areas, optimizing the lowest elevation angles respect to the obstacles close to the antenna. Provided an accurate 3D building reconstruction, airborne laser scanning data could be used to model the expected ground clutter return from the metropolitan area. Finally, simulating 3D obstacles, this methodology can be used to evaluate the impact on weather radar measurements of new buildings, infrastructures or changes in the urban areas close to the antenna.

Acknowledgements. This study has been supported by Academy of Finland (grant 263333) and the Academy of Finland Centre of Excellence (grant 272041). The authors would like to thank Matti Leskinen and Niko Tollman for the panoramic photo of the Helsinki skyline used in this paper.

References

Ahokas E., and Kaartinen, H., On the quality checking of the airbone laser scanning-based nation wide elevation model in Finland, 2013, available at: http://www.isprs.org/proceedings/xxxvii/congress/1_pdf/44.pdf, accessed 12.07.2014

Ackermann F., 1999: Airborne laser scanning—present status and future expectations, Isprs Journal of Photogrammetry and Remote Sensing, 54, 64-67, doi: 10.1016/S0924-2716(99)00009-X

Bean, B. R. and Dutton, E. J.: Radio Meteorology, Dover Publications, 435 pp., 1968.

Bech J., Codina B., Lorente J., and Bebbington D., 2003: The sensitivity of single polarization weather radar beam blockage correction to variability in the vertical refractivity gradient. J. Atmos. Oceanic Technol., 20, 845–855. doi: http://dx.doi.org/10.1175/1520-0426(2003)020<0845:TSOSPW>2.0.CO;2

Berne, A., Delrieu, G, Creutin, J., and Obed, C. (2004). Temporal and spatial resolution of rainfall measurements required for urban hydrology. Journal of Hydrology, 299, 166-179.

Dorninger, P., Pfeifer, N., 2008. A comprehensive automated 3D approach for building extraction, reconstruction, and regularization from airborne laser scanning point clouds. Sensors 8 (11), 7323–7343.

Doviak, R. J. and Zrnic, D. S., Doppler radar and weather observations. Academic Press Orlando, Fla, 1984.

Einfalt, T., Arnbjerg-Nielsen, K., Golz, C., Jensen, N.-E., Quirmbach, M., Vaes, G., et al. (2004) Towards a roadmap for use of radar rainfall data in urban drainage. J. Hydrol. 299, 186–202.

Fornasiero, A., Alberoni, P. P., and Bech, J., "Statistical analysis and modelling of weather radar beam propagation conditions in the Po Valley (Italy)," Nat. Hazards Earth Syst. Sci., vol. 6, no. 3, pp. 303 –314, May 2006. [Online]. Available: http://www.nat-hazards-earth-syst-sci.net/6/303/2006/

Fulton R.A., Breidenbach, J.P., D. Seo, D. Miller, and T. O'Bannon, 1998: The WSR-88D Rainfall Algorithm. Wea. Forecasting, 13, 377-395.

Giangrande, S. E. and A. V. Ryzhkov, 2005: Calibration of dualpolarization radar in the presence of partial beam blockage. J. Atmos. Oceanic Technol., 22:1156–1166

Guha-Sapir D., Below R., Ph. Hoyois - EM-DAT: The CRED/OFDA International Disaster Database - www.emdat.be - Université Catholique de Louvain – Brussels - Belgium. Accessed on 02/12/2016

Kada, M., McKinley, L., 2009. 3D building reconstruction from lidar based on a cell decomposition approach. International Archives of Photogrammetry, Remote Sensing and Spatial Information Sciences 38 (Part 3/W4), 47–52.

Kitchen, M., R. Brown, A.G. Davies, 1994: Real-time correction of weather radar data for the effects of bright band, range and orographic growth in widespread precipitation, Quart. J. Roy. Met. Soc., 120, 1231-1254.

Koskinen, J. T., Poutiainen, J., Schultz, D. M., Joffre, S., Koistinen, J., Saltikoff, E., Gregow, E., Turtiainen, H., Dabberdt, W. F., Damski, J., Eresmaa, N., Göke , S., Hyvärinen, O., Järvi, L., Karppinen, A., Kotro, J., Kuitunen, T., Kukkonen, J., Kulmala, M., Moisseev, D., Nurmi, P., Pohjola, H., Pylkkö, P., Vesala, T., and Viisanen, Y., "The helsinki testbed: A mesoscale measurement, ERAD 2014 Abstract ID 312 4ERAD 2014 - THE EIGHTH EUROPEAN CONFERENCE ON RADAR IN METEOROLOGY AND HYDROLOGY research, and service platform," Bulletin of the American Meteorological Society, vol. 92, no. 3, pp. 325-342, Mar 2011. [Online]. Available: http://dx.doi.org/10.1175/2010BAMS2878.1

Krajewski, W. F. , Ntelekos, A. A., and Goska, R., "A GIS-based methodology for the assessment of weather radar beam blockage in mountainous regions: Two examples from the US NEXRAD network," Comput. Geosci., vol. 32, no. 3, pp. 283–302, Apr. 2006. [Online]. Available: http://dx.doi.org/10.1016/j.cageo.2005.06.024

Kucera, W. F. K., Paul A. and Young, C. B., "Radar beam occultation studies using gis and dem technology: an example study of Guam," J. Atmos. Oceanic Technol, vol. 21, no. 3, pp. 995–1006, Apr. 2004.

Lang, T. J., S. W. Nesbitt, L. D. Carey, 2009: On the Correction of Partial Beam Blockage in Polarimetric Radar Data. J. Atmos. Oceanic Technol., 26, 943–957.

Marshall, J. S., and W. McK. Palmer 1948. The distribution of raindrops with size. J. Meteor. 5. 165–166.

Atmos. Meas. Tech. Discuss., doi:10.5194/amt-2016-76, 2016
Manuscript under review for journal Atmos. Meas. Tech.
Published: 18 March 2016

Atmospheric Measurement Techniques Discussions

QGIS Development Team, 2015. QGIS Geographic Information System. Open Source Geospatial Foundation Project. http://qgis.osgeo.org

Saltikoff E. 2012. Measuring Snow with Weather Radar. In Doppler Radar Observations, Bech J, Chau JL (ed.), Ch. 6, 159-174. Intech, Rijeka, Croatia. ISBN 978-953-51-0496-4 http://dx.doi.org/10.5772/2036 .

Saltikoff, E. and Nevvonen, L.: First experiences of the operational use of a dual-polarisation weather radar in Finland, Meteorol. Z., 20, 323–333, 2011.

Shan, J. and Sampath, A. , "Building extraction from LiDAR point clouds based on clustering techniques." Boca Raton, FL: CRC Press, 2008, pp. 423–446.

United Nations (2014). The World Urbanization Prospects: The 2014 Revision. The United Nations: New York. http://esa.un.org/UNPOP/wup/index.htm. accessed on 11 February, 2016.

United Nations International Office for Disaster Risk Reduction (UNISDR) (2011). Revealing Risk, Redefining Development. Global Assessment Report on Disaster Risk Reduction. Geneva, Switzerland: UNISDR.

Veldhuis, J.A.E. ten, Ochoa-Rodriguez, S., Bruni, G., Gires, A., Assel, J. van, Wang, L., Reinoso-Rodinel, R., Kroll S., Schertzer, D., Onof, C., Willems, P., Weather radar for urban hydrological applications: lessons learnt and research needs identified from 4 pilot catchments in North-West Europe, International Symposium – Weather Radar and Hydrology, Washington DC, April 2014

Vosselman, G., Dijkman S., 2001. 3D building model reconstruction from point clouds and ground plans. International Archives of Photogrammetry and Remote Sensing. 34(3/W4): 37–43.

Wood, C. R., Järvi, L., Kouznetsov, R. D., Nordbo, A., Joffre, S., Drebs, A., Vihma, T., Hirsikko, A., Suomi, I., Fortelius, C., O'Connor, E., Moiseev, D., Haapanala, S., Moilanen, J., Kangas, M., Karppinen, A., Vesala, T., and Kukkonen, J., "An overview of the urban boundary layer atmosphere network in helsinki," Bulletin of the American Meteorological Society, vol. 94, no. 11, pp. 1675–1690, Nov 2013. [Online]. Available: http://dx.doi.org/10.1175/BAMS-D-12-00146.1

Zhang P., Zrnić D., and Ryzhkov A., 2013: Partial beam blockage correction using polarimetric radar measurements. J. Atmos. Oceanic Technol., 30, 861–872. doi: http://dx.doi.org/10.1175/JTECH-D-12-00075.1

Atmos. Meas. Tech. Discuss., doi:10.5194/amt-2016-76, 2016
Manuscript under review for journal Atmos. Meas. Tech.
Published: 18 March 2016

Atmospheric Measurement Techniques Discussions

Table 1. Helsinki weather radar main characteristics.

Radar	Longitude	Latitude	Altitude	Beamwidth
Kumpula (KUM)	24.269° E	60.204° N	83 m	1.05°
Vantaa (VAN)	24.869° E	60.270° N	83 m	0.98°
Kerava (KER)	25.114° E	60.388° N	59 m	1.00°

Table 2. Kumpula weather radar partial beam blockages estimated from ALS data.

Location	Type	Azimuth	Distance(km)	Two-ways losses (dB)	
				0.5°	1.0°
Korskela Forsby	*chimney*	0°	1.5	1.42	*Free*
Hanasaari	*power plan chimneys*	169° - 170°	2.0	2.28 – 3.98	< 1
Paavalin Kirkko	*bell tower*	192°- 193°	0.8	1.38 - 4.42	< 1
Kallion Kirkko	*bell tower*	199°	2.4	1.92	*Free*
Linnanmäki	*amusement park*	216°	2.1	2.38	*Free*
Itä-Pasila	*residential area*	236°	1.3	4.52	*Free*
Itä-Pasila	*residential area and mast*	240°, 245°	1.6 -1.7	1.00 – 2.84	1.69
Itä-Pasila	*residential area and two masts*	247° - 249°	1.6-1.7	1.19-2.04	*Free*
Itä-Pasila	*residential area*	252° - 253°	1.4	5.56 – 6.02	*Free*
YLE Studiotalo	*industrial buildings*	265° - 267°	2.4	1.24 – 3.95	*Free*
YLE Studiotalo	*television tower*	270° - 271°	2.2	1.58 - 6.36	5.13
Ilmala	*industrial buildings*	275° - 277°	2.6	1.34 - 2.94	*Free*
Central Park	*trees and mast*	304° - 310°	3.1	1.00 - 1.18	*Free*
Käpylä	*residential area and trees*	333° - 347°	1.8 - 2.0	0.99 – 2.28	*Free*

Table 3. Kumpula weather radar two-ways losses at 0.5° elevation: comparison estimated values from ALS data and observed ones derived by 24-hours accumulation rainfall. Gray shaded rows reports anomalies that are discussed in the text.

Location	Type	Azimuth	Distance(km)	Two-ways losses @0.5° (dB)	
				Estimated	Observed
Korskela Forsby	*chimney*	0°	1.5	1.42	2.2
Hanasaari	*power plan chimneys*	169° - 170°	2.0	3.98	1.8
Paavalin Kirkko	*bell tower*	192°- 193°	0.8	4.42	3.2
Linnanmäki	*amusement park*	216°	2.1	2.38	1.8
Itä-Pasila	*residential area*	236°	1.3	4.52	5.5
Itä-Pasila	*residential area and mast*	240°, 245°	1.6 -1.7	2.84	2.9
Itä-Pasila	*residential area and two masts*	247° - 249°	1.6 -1.7	2.04	9.1
Itä-Pasila	*residential area*	252° - 253°	1.4	6.02	8.7
YLE Studiotalo	*industrial buildings*	265° - 267°	2.4	3.95	2.44
YLE Studiotalo	*television tower*	270° - 271°	2.2	6.36	4.09
Ilmala	*industrial buildings*	275° - 277°	2.6	2.94	4.28
Käpylä	*residential area and trees*	333° - 347°	1.8 - 2.0	2.28	2.34

Atmos. Meas. Tech. Discuss., doi:10.5194/amt-2016-76, 2016
Manuscript under review for journal Atmos. Meas. Tech.
Published: 18 March 2016

Atmospheric Measurement Techniques Discussions

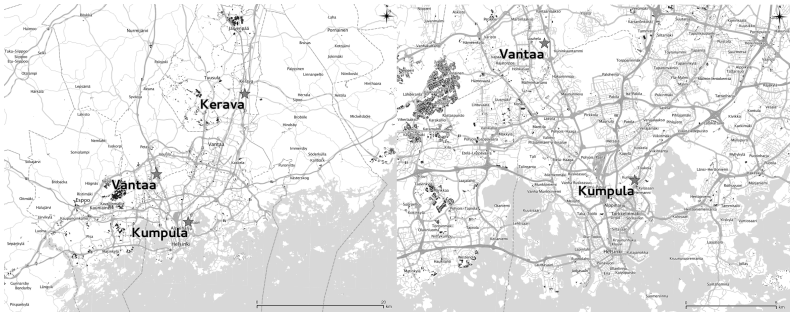

Figure 1. The weather radar locations within metropolitan area of Helsinki, Finland: Left: the map overview of the three radar sites. Right: the detailed map for Vantaa and Kumpula radar indicating main roads, railways and buildings.

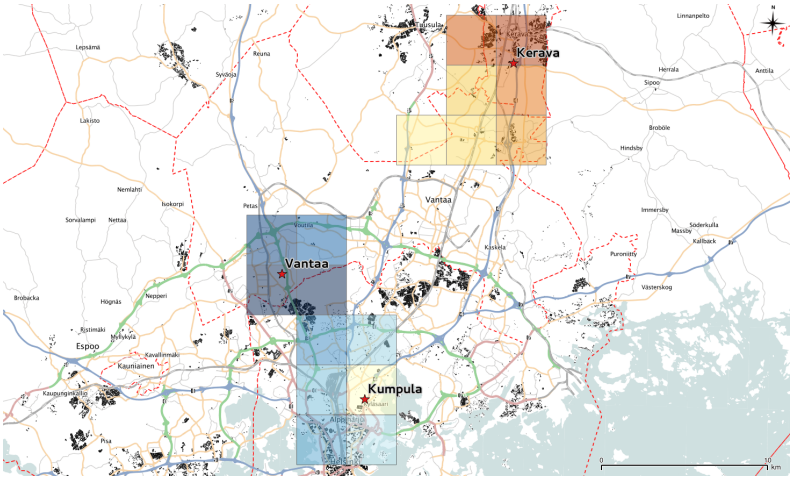

Figure 2. The ALS data tiles considered in this study.

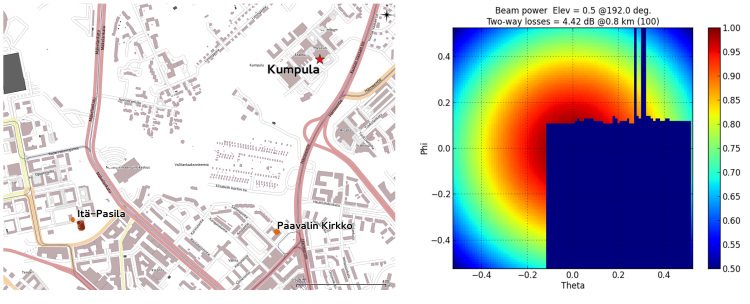

Figure 3. Left: the Kumpula radar and the bell tower map, Helsinki. Right: estimated radar beam blocking at 0.7° elevation and 192° azimuth. Colour represents the beam power normalized to one in the beam center

Atmos. Meas. Tech. Discuss., doi:10.5194/amt-2016-76, 2016
Manuscript under review for journal Atmos. Meas. Tech.
Published: 18 March 2016

Atmospheric Measurement Techniques Discussions

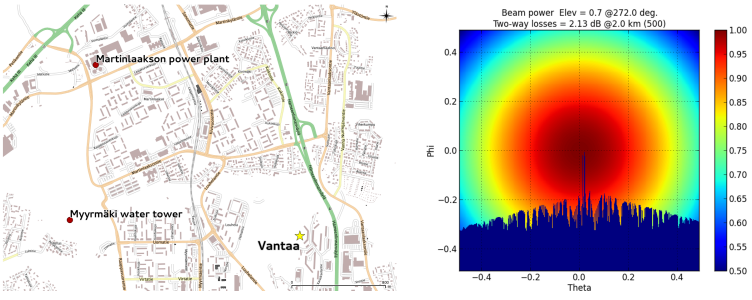

Figure 4. Left: Vantaa radar and Myyrmäki water tower. Right: estimated radar beam blocking at 0.7° elevation and 272° azimuth. Colour represents the beam power normalized to one in the beam centre.

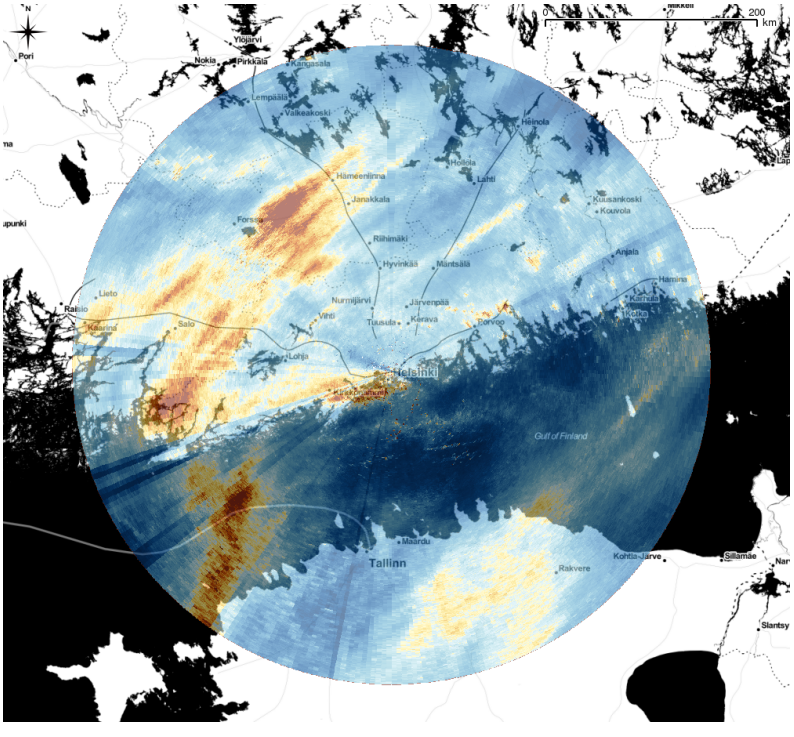

Figure 5. 24-hours rainfall accumulation on September 22, 2014 from Kumpula PPI reflectivity @0.5° elevation

Atmos. Meas. Tech. Discuss., doi:10.5194/amt-2016-76, 2016
Manuscript under review for journal Atmos. Meas. Tech.
Published: 18 March 2016

Atmospheric Measurement Techniques Discussions

Figure 6. Left: Itä-Pasila partial beam-blockage. Lines show beam centre path for 252°, 248° amd 240° azimuths; dots are ALS data, and colours correspond to altitude above sea level (brown 60 m, yellow 65 m, orange 70 m, red 75 m and purple > 75 m). The two masts and a flag-pole along the beam path are also reported. Right: Google street map view of the two masts from Böle bro (Itä-Pasila, Helsinki. Map. Google Street. Google, Jun 2009. Web. 3 Feb 2016).

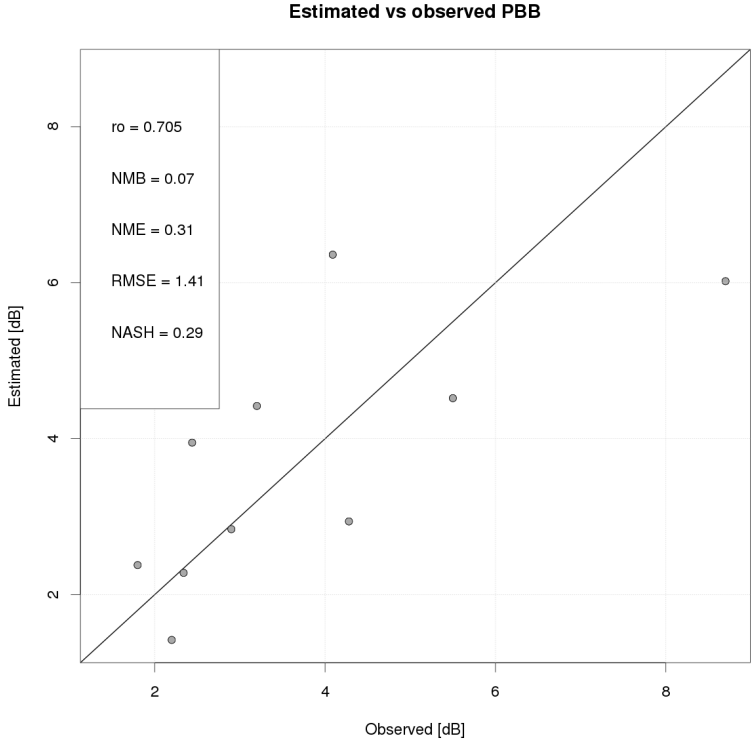

Figure 7. The scatter plot between laser scanning-based estimated two-way losses and observed ones for Kumpula radar with 0.5° elevation. Ro is the Pearson correlation coefficient, NMB the normalized mean bias, NME the normalized mean error, RMSE the root mean square error and NASH the Nash–Sutcliffe model efficiency coefficient.

Atmos. Meas. Tech. Discuss., doi:10.5194/amt-2016-76, 2016
Manuscript under review for journal Atmos. Meas. Tech.
Published: 18 March 2016

Atmospheric Measurement Techniques Discussions

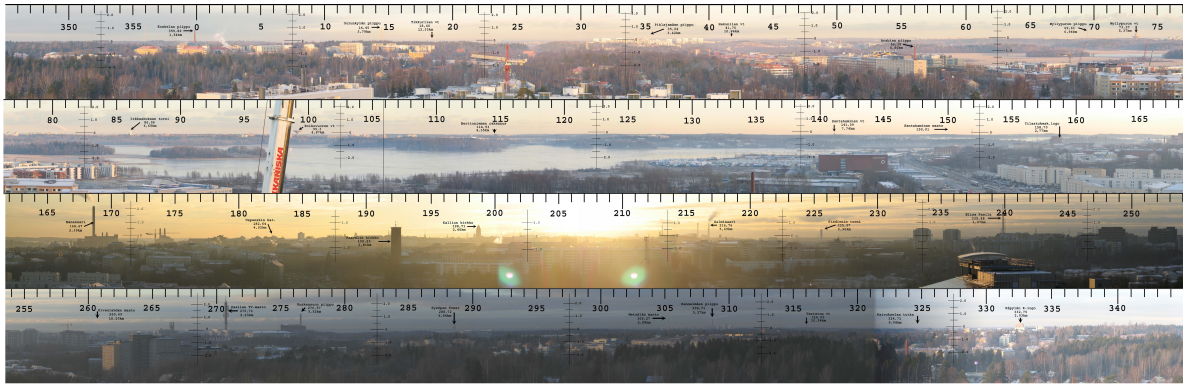

Figure 8. The 360° panoramic view from the antenna tower of Kumpula radar.